Multifunctional gold nanorods for image-guided surgery and photothermal therapy

Clement Barriere*, Ji Qi, P. Beatriz Garcia Allende, Richard Newton, Daniel S. Elson

The Hamlyn Centre for Robotic Surgery, Department of Surgery and Cancer, Imperial College London, London SW7 2AZ
*Corresponding Author: c.barriere@imperial.ac.uk

ABSTRACT

Nanoparticles are viewed as a promising tool for numerous medical applications, for instance imaging and photothermal therapy (PTT) has been proposed using gold nanorods. We are developing multi-functional gold nanorods (m-GNRs) which have potential for image guided endoscopic surgery of tumour tissue with a modified laparoscope system. A new synthesis method potentially allows any useful acid functionalised molecules to be bonded at the surface. We have created fluorescent m-GNRs which can be used for therapy as they absorb light in the infrared, which may penetrate deep into the tissue and produce localised heating. We have performed a tissue based experiment to demonstrate the feasibility of fluorescence guided PTT using m-GNRs. *Ex vivo* tests were performed using sheep heart. This measurement, correlated with the fluorescence signal of the m-GNRs measured by the laparoscope allows the clear discrimination of the artery system containing m-GNRs. A laser diode was used to heat the m-GNRs and a thermal camera was able to record the heat distribution. These images were compared to the fluorescence images for validation.

Keywords: Gold Nanorods, Photothermal Therapy, Imaging, Multifunctional Nanoparticles

1. INTRODUCTION

During the last ten years, gold nanoparticles have been a subject of high interest for their unique combination of physical, chemical and biological properties[1,2]. In particular, nanoparticles showing a strong absorption of light in the infrared (IR) have generated considerable recent research interest[3,4], and could be a new tool for the imaging and therapy of cancer[5]. Among these, gold nanorods (GNRs) have received attention as their synthesis and its corresponding properties are well documented[6]. In the field of medicine, GNRs have already generated numerous studies with various imaging techniques applied (photoacoustic tomography[7-9], X-rays[10], darkfield spectroscopy[11] and two photon luminescence[12]), as well as photothermal therapy by finely adjusting the optical properties and function[13-15]. Unfortunately, there are only limited examples of GNRs specifically designed for imaging and therapy. In this study, a new chemical route for the synthesis of nanoconstructs has been designed, involving the use of a bifunctional polyethylene glycol (PEG) combined with various carboxylic acids to produce multifunctional gold nanorods (m-GNRs). Those particles have then been injected in sheep ex-vivo tissue and their fluorescent and heating properties have been tested.

2. EXPERIMENTAL METHODS

2.1 Reagents and materials

All chemicals were purchased from Sigma-Aldrich, except from the two amine-thiol polyethylene glycols (PEG) which were purchased from Cheshire Sciences. All biological media and reagents were purchased from Invitrogen. We used an IR laser diode (ThorLabs, L808P1WJ, 808 nm, maximum power: 1W) to heat the GNRs and a thermal camera (FLIR S65 thermal imaging camera - 320×240 pixel LWIR detector - 80mK) to detect the corresponding heat. A 10 mm diameter 0 degree rigid laparoscope was used to detect the fluorescence.

2.2 Synthesis and coating of m-GNRs

The GNRs were synthesised following the method described by Seo *et al.*[16]. A UV spectrophotometer (Jasco V630) was used to monitor the GNR size by observation of the characteristic deep absorption peak around 800 nm, and the size was subsequently confirmed using a Jeol 2010 transmission electronic microscope. One hour

after the beginning of the synthesis, the solution was cooled down to 4°C to precipitate a part of the large excess of CTAB, which was then filtered.

To functionalise the GNRs, a simple, bio-compatible and reproducible technique was developed. It is a two-step method consisting first of the protection of the GNRs with a polyethylene glycol (PEG) followed by the addition of one or more carboxylic acid(s), as presented in the following sections.

2.2.1 Protection of the GNRs using PEG

Three commercial PEGs have been tested, as shown in table 1. In a standard experiment, a 5 mL solution of GNRs was synthesised and filtered as described above was centrifuged at 8500 rpm for 15 minutes (Eppendorf 5804R) in a centrifuge tube. The supernatant was removed and 2 µmol of PEG was dissolved in 0.5 mL of PBS (Phosphate buffered saline). The centrifuge tube was then strongly stirred on a vortex mixer (Fisher Scientific ZX Classic) for 10 seconds and then put on a roller mixer (Stuart Scientific SRT1) for one hour. One PEG type ($SH\text{-}PEG_{1000}\text{-}CH_3$) could not be functionalised any further and was synthesised for testing purposes only.

Name	$SH\text{-}PEG_{1000}\text{-}CH_3$	$SH\text{-}PEG_{3400}\text{-}NH_2$	$SH\text{-}PEG_{5000}\text{-}NH_2$
Structure	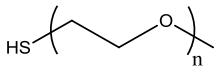	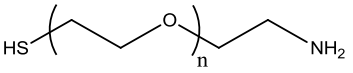	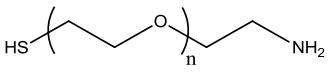
M_w (g/mol)	1000	3400	5000

Table 1: Polymers used for the functionalization of the GNRs

The same PEG could also be synthesised in the lab starting from the bis-amine PEG (M_w = 1500 g/mol) and Traut's Reagent (TR) as shown below:

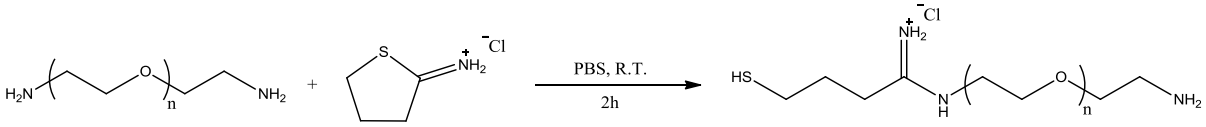

Figure 1: Synthesis of thiol-amino PEG

TR is known for the monothiolation of bisamine[17], and has already been used for the functionalization of similar materials in similar conditions[18]. In a standard experiment, 2 µmol of bis-amine PEG was dissolved in 0.5 mL of PBS and then mixed with 2 µmol of TR (which was also prepared in a solution of PBS for a better accuracy). After two hours, the solution was mixed with the nanoparticles as explained above. Note that to improve stability it was necessary to add 1 µmol of the $SH\text{-}PEG_{1000}\text{-}CH_3$ to this solution.

2.2.2 Addition of carboxylic acid

The same method was used for all different carboxylic acids (carminic acid, folic acid and fluorescein). Firstly, the activated form of the acid was prepared as shown below:

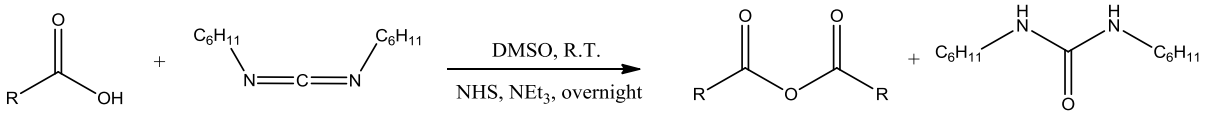

Figure 2: Activation of acids with a carbodiimide

In a standard procedure, 0.23 mmol of acid was dissolved in 2 mL of dry DMSO. Then reagents were added in this order: 50 µL of triethylamine, 52 mg of NHS (N-Hydroxysuccinimide) and finally 94 mg of DCC (N,N'-Dicyclohexylcarbodiimide). The solution was stirred overnight. Post treatment consisted of the filtration of solution followed by the precipitation of the final product in ether. Details can be found in previous work in the literature[17]. The precipitate can be kept in a freezer at -20°C for a couple of weeks only as it quickly react with water and degrade, and is usually directly used on the nanoparticles after synthesis.

The reaction of these activated acids with the GNRs is performed as shown in Figure 3. Briefly, a large excess of the activated acid (100 µmol, in a minimum quantity of dry DMSO) was added to the PEG-GNRs (a solution prepared as described above which was previously buffered at pH = 8 with Na_2CO_3). In the case of the addition

of multiple acids, all were added simultaneously to the solution (equal quantities of each acid were chosen so that the total quantity of acid was still 100 µmol). As presented above, the centrifuge tube was then strongly stirred on the vortex mixer for 10 seconds, and afterwards was left for two hours on the roller mixer. Finally, the solution was centrifuged at 8500 rpm for 15 minutes. The supernatant was removed, and the solution was stirred and centrifuged one more time in the same conditions before its use.

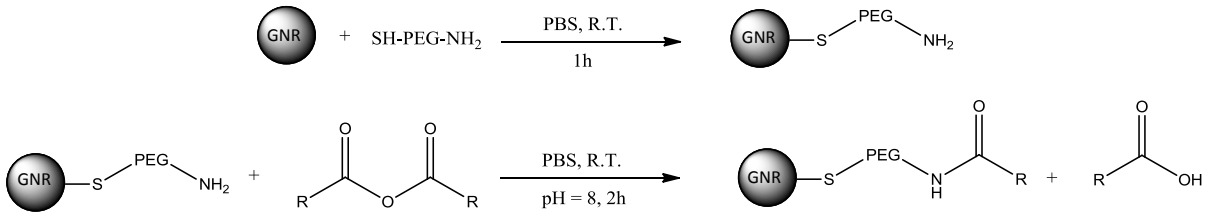

Figure 3: GNRs modification synthesis

2.3 Experiments on tissue

This experiment was designed to demonstrate the feasibility of the localised image-guided PTT in tissue using fluorescence. The experimental set-up is shown in figure 4. Fresh tissue samples (lungs, heart and bowel) were taken just after the sheep termination. A solution of m-GNRs was injected in the tissue *via* an artery after the removal of the blood. The nanoparticle solution was allowed to progress along the artery. In a standard experiment, samples were held by a clamp and tissue was imaged with the laparoscope and illuminated through the illumination channel with a red, green, blue LED endoscopic illuminator for white light imaging, and just the blue LED to excite fluorescence of the tissue before and after the injection of m-GNRs. More information on this new LED system can be found in another study from our group[19]. We also used a thermal camera to detect the heat produced by the application of the laser at 808 nm with the beam focused on the artery (circle of diameter around 1cm).

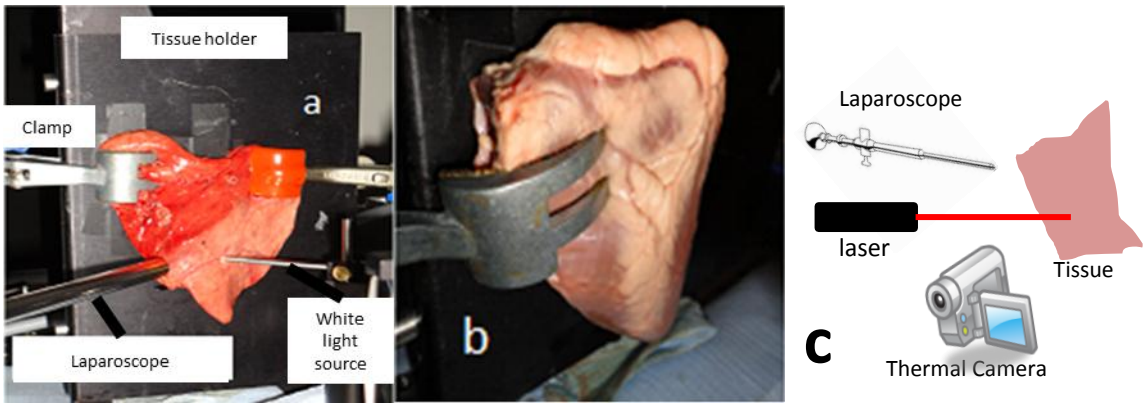

Figure 4: Sheep lungs (a) and heart (b) and set-up used for the experiment (c)

3. RESULTS

3.1 Fluorescence study

In a previous study we used reflectance spectroscopy to detect m-GNRs on and inside a tissue (chicken breast)[20]. Here we present some results on fluorescence detection and laser heating on sheep tissue (heart, lungs and bowel. Figure 5 displays the fluorescence of the fluorescein of the m-GNRs in lungs. The tissue reflectance is seen with a time exposure of six seconds whereas the m-GNRS allowed the detection of the blood vessels that had been injected with the nanoparticle solution, with an exposure time of 2.22 seconds and despite the thickness of the vessel walls.

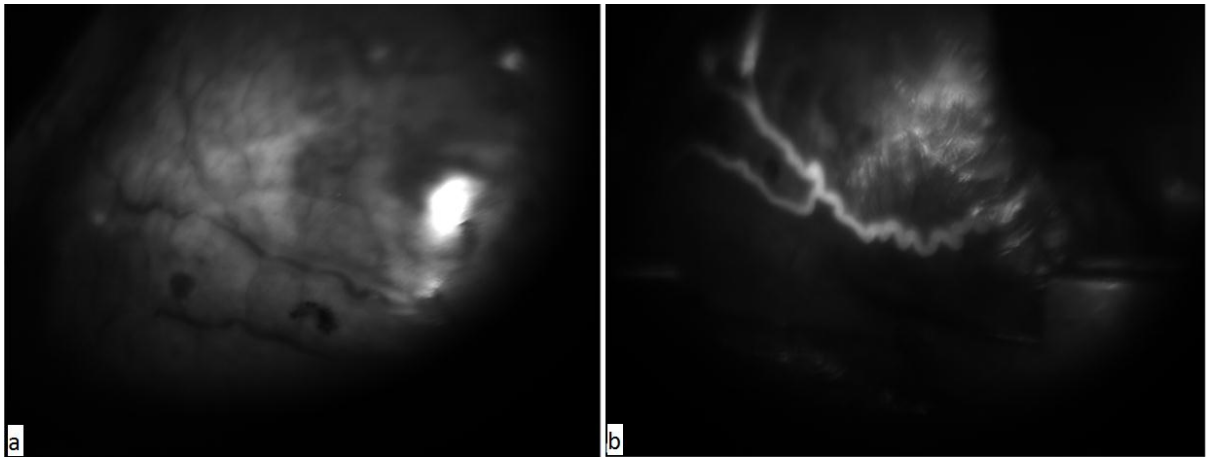

Figure 5: Fluorescence pictures using the laparoscope a) without the m-GNRs. b) with the m-GNRs.

These results could be easily reproduced in the heart and the intestine tissue and suggests that a similar approach could be used in the determination of the presence or absence of tumour using a targeted fluorescent agent, particularly with infrared fluorescence.

3.2 Photothermal therapy

We also assessed the heating potential of m-GNRs through the tissue. Figure 6 compares the temperature profiles of the heart after 92 seconds of laser heating in both the presence and absence of particles. To detect the increase of temperature, we used a thermal camera, although the temperature given here is underestimated as the camera can only detect the surface temperature. It is also worth noting that the temperature given on the picture is calculated depending on the emissivity value. This value (experimentally calculated in our case of 0.7 for the tissue) is the same for the entire picture; even though it highly depends on the physical nature on an object (*e.g.* the metal clamp appears hotter than the plastic background and the tissue).

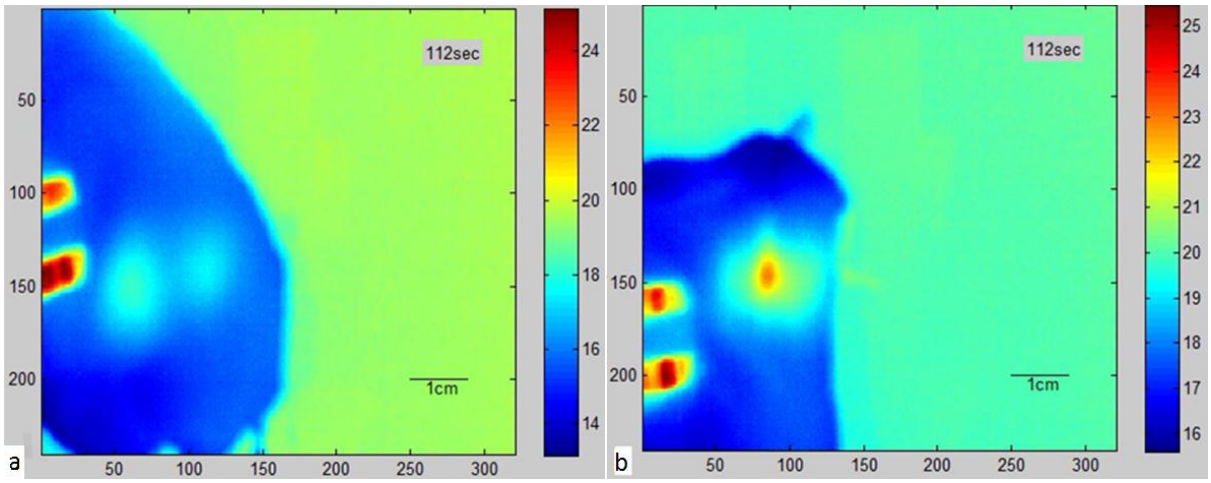

Figure 6: Thermal camera images of tissue heating by a laser a) in absence and b) in presence of m-GNRs.

From figure 6a) only a weak rise of temperature could be detected with the thermal camera on the surface, which is in this case the hottest part of the tissue. On the contrary, figure 6b) displays a significant colour change due to the heat created by the m-GNRs inside the blood vessel. It also reveals that the heat is relatively localised to the blood vessel and decreases rapidly with distance. These pictures provide evidence that the heating is localised within the blood vessel.

4. DISCUSSION

We have synthesised multifunctional nano-constructs which are able to present various different properties for one single object. This includes fluorescence and the heating abilities. The toxicity *in vitro* has been studied through two different techniques not presented here, providing initial evidence that the main toxicity can be

addressed by controlling the surface layer of the particles. Further work is required to assess the toxicity depending on the total or partial coverage of the amine function with the carboxylic acids. A correlation of this toxicity with the zeta-potential value of the m-GNRs will also be attempted. Using an IR-laser, we have demonstrated the feasibility to create a significant increase of the temperature locally to provoke cell death, both *in vitro* in a bulk tissue. Finally, fluorescence can be detected through the tissue using fluorescent modified nanoparticles. Further work will include the identification the quantity of energy required to create local apoptosis of the cells in a tissue without necrosis and without spread of spread of heat to the surrounding healthy cells, which will involve small animal work. These results demonstrate the potential of multifunctional nano-constructs for image guided detection and therapy of tumours.

ACKNOWLEDGMENTS

Funding for this work was provided by ERC grant 242991. The authors would like to thank Professor George Hanna (ICL, Department of Surgery and Cancer) for the loan of the thermal camera.

REFERENCES

[1] Shan, J., and Tenhu, H., "Recent advances in polymer protected gold nanoparticles: synthesis, properties and applications," Chem. Commun. 44, 4580-4598 (2007).

[2] Daniel, M.-C., and Astruc, D. Gold Nanoparticles, "Assembly, Supramolecular Chemistry, Quantum-Size-Related Properties, and Applications toward Biology, Catalysis, and Nanotechnology," Chem. Rev. 104(1), 293-346 (2004).

[3] Link, S., and El-Sayed, M. A., "Shape and size dependence of radiative, non-radiative and photothermal properties of gold nanocrystals," Int. Rev. Phys. Chem. 19(3), 409-453 (2000).

[4] Norman, T. J. Jr., Grant, C. D., and Zhang, J. Z., Nanoparticle Assemblies and Superstructures. CRC Press Online, Ann Arbor (2005).

[5] Huang, X., Jain, P. K., El-Sayed, I. H., and El-Sayed, M. A., "Gold nanoparticles: interesting optical properties and recent applications in cancer diagnostics and therapy," Nanomedicine 2(5), 681-693 (2007).

[6] Huang, X., Neretina, S., and El-Sayed, M. A., "Gold Nanorods: From Synthesis and Properties to Biological and Biomedical Applications," Adv. Mater. 21(48), 4880-4910 (2009).

[7] Song, K. H., Kim, C., Maslov, K., and Wang, L. V., "Noninvasive in vivo spectroscopic nanorod-contrast photoacoustic mapping of sentinel lymph nodes," Eur. J. Radiol. 70(2), 227-231 (2009).

[8] Chen, Y.-S., Frey, W., Kim, S., Homan, K., Kruizinga, P., Sokolov, K., and Emelianov, S., "Enhanced thermal stability of silica-coated gold nanorods for photoacoustic imaging and image-guided therapy," Opt. Express 18(9), 8867-8878 (2010).

[9] Galanzha, E. I., Kokoska, M. S., Shashkov, E. V., Kim, J.-W., Tuchin, V. V., and Zharov, V. P., "In vivo fiber-based multicolor photoacoustic detection and photothermal purging of metastasis in sentinel lymph nodes targeted by nanoparticles," J. Biophotonics 2(8-9), 528-539 (2009).

[10] Wang, L., Li, Y.-F., Zhou, L., Liu, Y., Meng, L., Zhang, K., Wu, X., Zhang, L., Li, B. and Chen, C., "Characterization of gold nanorods in vivo by integrated analytical techniques: their uptake, retention, and chemical forms," Anal. Bioanal. Chem. 396(3), 1105-1114. (2010).

[11] Xiao, L., Qiao, Y., He, Y. and Yeung, E. S, "Three Dimensional Orientational Imaging of Nanoparticles with Darkfield Microscopy," Anal. Chem. 82(12), 5268-5274 (2010).

[12] Zhu, J., Yong, K.-T., Roy, I., Hu, R., Ding, H., Zhao, L., Swihart, M. T., He, G. S., Cui, Y. and Prasad, P. N., "Additive controlled synthesis of gold nanorods (GNRs) for two-photon luminescence imaging of cancer cells," Nanotechnology 21(28), 285106-285113 (2010).

[13] Park, J.-H., Maltzahn, G. von, Ong, L. L., Centrone, A., Hatton, T. A., Ruoslahti, E., Bhatia, S. N. and Sailor, M. J., "Cooperative Nanoparticles for Tumor Detection and Photothermally Triggered Drug Delivery," Adv. Mater. 22(8), 880-885 (2010).

[14] Li, Z., Huang, P., Zhang, X., Lin, J., Yang, S., Liu, B., Gao, F., Xi, P., Ren, Q. and Cui, D., "RGD-Conjugated Dendrimer-Modified Gold Nanorods for in Vivo Tumor Targeting and Photothermal Therapy," Mol. Pharmaceutics 7(1), 94-104 (2010).

[15] Huang, H.-C., Rege, K., and Heys, J. J., "Spatiotemporal Temperature Distribution and Cancer Cell Death in Response to Extracellular Hyperthermia Induced by Gold Nanorods," ACS Nano 4(5), 2892-2900 (2010).

[16] Seo, S. S., Wang, X., and Murray, D., "Direct monitoring of gold nanorod growth," Ionics 15(1), 67-71 (2009).

[17] Traut R. R., "Methyl 4-mercaptobutyrimidate as a cleavable cross-linking reagent and its application to the Escherichia coli 30S ribosome," Biochem. 12, S. 3266–3273 (1973).

[18] Gabizon, A., Shmeeda, H., Horowitz, A. T., and Zalipsky, S., "Tumor cell targeting of liposome-entrapped drugs with phospholipid-anchored folic acid-PEG conjugates," Adv. Drug Delivery Rev. 56(8), 1177-1192 (2004).

[19] Clancy, N. T., Li R., Rodgers, K., Driscoll, P., Excell, P., Yandle, R., Hanna, G. B., Copner, N. and Elson, D. S., "Development and evaluation of a light-emitting diode endoscopic light source," Proc. SPIE 8214, 8214-27 (2011).

[20] Garcia-Allende, P. B., Barriere, C., Sauvage, V. S., Qi, J., and Elson, D. S., "Method to determine optimal illumination wavelengths for gold nanoparticle detection in tissue using reflectance spectroscopy," Proc. SPIE 8087, 80872L-80872L-8 (2011).